

# Microdynamics and Criticality in Evolving Random Graphs

Ben D. MacArthur,<sup>1,\*</sup> Rubén J. Sánchez-García,<sup>2</sup> and Avi Ma'ayan<sup>1</sup>

<sup>1</sup>*Department of Pharmacology and Systems Therapeutics,*

*Systems Biology Center New York (SBCNY), Mount Sinai School of Medicine, New York, NY, USA.*

<sup>2</sup>*Mathematisches Institut, Heinrich-Heine Universität Düsseldorf, Universitätsstr 1, 40225, Düsseldorf, Germany.*

(Dated: September 3, 2022)

We present a simple evolutionary model which couples structural rearrangement in signed directed graphs to dynamic stability. The resulting graphs exhibit a stationary heavy-tailed degree distribution. However, this macroscopic stationarity masks complex equilibrium ‘microdynamics’ in which individual nodes continually accumulate and lose links. This structural microdynamics, in turn, gives rise to complex global dynamical state characterized by periods of stability interrupted by intermittent bursts of instability (‘punctuated equilibrium’). By deriving analytic relationships between cyclic structure and stability in signed digraphs, we show that the observed bursting dynamics result primarily from the continual formation and breaking of transient directed cycles during the evolutionary process. At equilibrium, bursts of instability develop heavy-tailed statistics, indicating a possible self-organized critical state.

PACS numbers: 89.75.-k, 89.75.Fb, 02.10.Ox, 05.65.+b

*Introduction.*— A great deal of recent research attention has been focused on understanding the structure of naturally occurring empirical networks and associated random graph models [1, 2]. An overarching aim of many of these studies has been to determine the relationships between network structure and dynamics. For instance, the presence of modularity and sparsity have long been known to contribute to global stability [3] while the presence of some kind of feedback (cyclic structure) is a well-studied prerequisite for the support of complex dynamics such as oscillations, multistability and chaos [4].

Although much work has, so far, focused on ‘static’ networks, many real-world complex systems evolve both structurally and dynamically over time. For this reason *coevolutionary* systems – in which structure and dynamics coevolve – have begun to attract increasing research interest (see [5] and references therein). An emerging theme of these studies is that feedback between structure and dynamics can give rise to complex patterns of behavior not observed when structure and dynamics are decoupled [6].

Here we outline a simple evolutionary model which couples structural changes in signed directed graphs to their dynamic stability and, by so doing, reproduces both structural and dynamic features of naturally occurring complex systems. In particular, the resulting graphs exhibit a characteristic stationary heavy-tailed degree distribution, show complex structural microdynamics and organize to a dynamically critical state.

*Preliminaries.*— We begin with a few necessary definitions. Mathematically a network is a graph consisting of a set of vertices (or nodes)  $V$  (of size  $n$ ) and a set of edges (or links)  $E$ . A directed graph (digraph) is a graph in which each edge  $v_i \sim v_j \in E$  has a unique orienta-

tion ( $v_i \rightarrow v_j$ ). Although digraphs describe well structural relationships in complex systems, in many cases relationships also have an intrinsic sign – friendship and enmity in social networks or activation and inhibition in biochemical regulatory networks, for instance. To cope with such systems a natural framework is that of signed digraphs [7]. A signed digraph  $\vec{S}$  is a digraph in which each edge  $v_i \sim v_j \in E$  additionally has a unique sign  $\sigma_{ij} \in [-1, +1]$  depending on whether it is ‘activating’ ( $\sigma_{ij} = +1$ ) or ‘inhibiting’ ( $\sigma_{ij} = -1$ ). The adjacency matrix  $\mathbf{A} = a_{ij}$  of a signed digraph has the form  $a_{ij} = \sigma_{ij}$  if  $v_i \sim v_j \in E$  and  $a_{ij} = 0$  otherwise. When considering structural features of  $\vec{S}$  without regard for signs we shall also make use of the absolute adjacency matrix  $\tilde{\mathbf{A}} = |a_{ij}|$ . The in-degree (out-degree) of a vertex is the number of in-coming (out-going) edges it has, without regard for sign. The net-degree  $d_{\text{net}}(v_i) = |d_{\text{in}}(v_i) - d_{\text{out}}(v_i)|$  of a vertex  $v_i$  as the absolute difference of its in-coming and out-going degree. Intuitively, net-degree measures how ‘source-’ or ‘sink-’ like a vertex is. By extension, we define the *imbalance* of a vertex-pair as the absolute difference of their net-degrees,  $I(v_i, v_v) = |d_{\text{net}}(v_i) - d_{\text{net}}(v_v)|$ . It has recently been observed that many empirical networks contain significantly more source and sink nodes than expected by chance, and that this degree imbalance naturally leads to depletion of feedback loops (cycles) which, in turn, confers enhanced stability properties [8]. Thus, degree imbalance and dynamic stability are intrinsically related, a fact that our model seeks to exploit.

*Model.*— We begin at  $t = 0$  with a random signed digraph  $\vec{S}(t = 0)$  of size  $n$  with Erdős-Rényi connectivity, in which edge orientations and signs have been assigned independently in an equiprobable random manner [21]. We then rewire  $\vec{S}(t)$  at successive time-steps according to the following rules: (1) randomly and uniformly chose an edge  $e_{\text{old}} = v_a \sim v_b$  connecting two vertices in  $\vec{S}(t)$  such that  $\vec{S}(t) - e_{\text{old}}$  is not disconnected and an ordered

\*Electronic address: ben.macarthur@mssm.edu

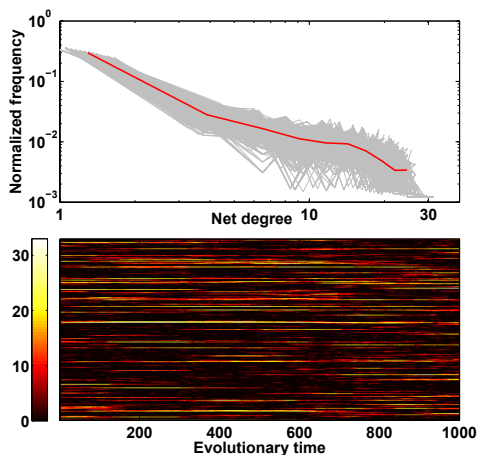


Figure 1: Graphs resulting from the evolutionary process exhibit a stationary heavy-tailed degree distribution. (*Top*) The net-degree distribution at 1000 time-step intervals for a period of  $1 \times 10^6$  time-steps at equilibrium for a 250 vertex graph are shown in light gray. In bold (red online) is the mean net-degree distribution over this time period. (*Bottom*) Each row shows the changing net-degree of one vertex. Note that vertices continually accumulate and lose links during the evolutionary process, indicating complex ongoing structural microdynamics.

pair of non-adjacent vertices  $v_c, v_d \neq v_c$ . (2) Calculate the pair-wise imbalances  $I(v_a, v_b)$  and  $I(v_c, v_d)$ . (3) Delete  $e_{\text{old}}$  and create a new edge  $e_{\text{new}} = v_c \rightarrow v_d$ , choosing its sign  $\pm 1$  randomly with probability  $1/2$ , and recalculate the imbalances. (4) If the sum of the two imbalances after the switch is greater than that before then accept the switch unconditionally, otherwise accept with probability  $\rho(t)$ , as described below.

In order to couple structural rearrangement to dynamics we allow  $\rho(t)$  to vary in a manner which takes into account the changing stability of the system. To do so we assume that, in addition to regulatory links defined by  $\vec{S}(t)$ , each species (vertex  $v_i$ ) also dissipates (or decays) at a constant characteristic rate  $\epsilon_i$  which we fix at  $t = 0$  independently, randomly and uniformly on the unit interval (that is, we set  $\epsilon_i \in [0, 1]$  for all  $i = 1 \dots n$ ). Thus, at each evolutionary time-point we obtain a modified adjacency matrix  $\mathbf{B}(t) = \mathbf{A}(t) - \text{diag}(\epsilon_i)$ . Global stability is then given by the magnitude of  $\mu_{\text{max}}(t) = \max \text{Re } \mu_i(t)$ , where  $\mu_i(t)$  for  $i = 1 \dots n$  are the eigenvalues of  $\mathbf{B}(t)$ . In particular, the system is stable when  $\mu_{\text{max}}(t) < 0$  and unstable when  $\mu_{\text{max}}(t) > 0$ . Therefore we set  $\rho(t) = 1 - h[\mu_{\text{max}}(t)]$ , where  $h[x]$  is the Heaviside step function, allowing defective switches when the system is stable and suppressing defective switches when the system is unstable. The key property of this coupling is that it makes global information available to the local structural reorganizing process, providing continual feedback between structure and dynamics.

*Results.*— The graphs produced by this simple model

are characterized by a stationary heavy-tailed degree distribution (see Fig. 1 top panel) indicating the presence of hub source and sink vertices, a well-known feature of real-world networks [8, 9]. However, since our model allows for periods of random structural rearrangement, this macroscopic stationarity masks complex structural ‘microdynamics’ in which individual vertices continually accumulate and lose edges and rise and fall in their centrality (see Fig. 1 bottom panel). This kind of structural microdynamics is not produced by classical rich-get-richer models of hub formation [9], but has recently been highlighted as an important characteristic of real-world evolving (macroscopically stationary) complex networks [10, 11].

Fig. 2 gives a plot of  $\mu_{\text{max}}(t)$  at equilibrium [22] for a representative system showing that dynamics on the evolutionary time-scale are characterized by periods of stability ( $\mu_{\text{max}}(t) < 0$ ) punctuated by bursts of instability ( $\mu_{\text{max}}(t) > 0$ ). To help interpret these dynamics, also shown is  $\lambda_{\text{max}}(t) = \max \text{Re } \lambda_i(t)$ , where  $\lambda_i(t)$  are the eigenvalues of the graph adjacency matrix  $\mathbf{A}(t)$  (see comments later) and three measures of graph structure. The first structural measure shown is total net-degree  $D_{\text{net}}(t) = \sum_i d_{\text{net}}[v_i(t)]$ , a measure of overall degree imbalance in  $\vec{S}(t)$ . It is apparent that changes in total net-degree correlate poorly with changes in stability. In particular, total net-degree does not exhibit bursting behavior, suggesting that although fluctuations in net-degree are observed during the evolutionary process, it is not degree-imbalance *per se* that drives the characteristic dynamics of  $\mu_{\text{max}}(t)$ . In order to identify more precisely the structural origin of bursts of instability, and based upon the observation that degree imbalance naturally leads to feedback loop depletion [8], also shown are two measures of network cyclic structure [23]. The first,  $\Phi(t) = n_{\text{cyc}}(t)/n$  where  $n_{\text{cyc}}(t)$  is the number of vertices which participate in a cycle in  $\vec{S}(t)$ , measures overall cyclic structure without regard for details such as cycle numbers or distribution of cycle lengths. The second,

$$\Psi(t) = \text{Trace } e^{\tilde{\mathbf{A}}(t)} - n = \sum_{i=1}^n e^{\tilde{\lambda}_i(t)} - n, \quad (1)$$

where  $\tilde{\lambda}_i$  are the eigenvalues of the absolute adjacency matrix  $\tilde{\mathbf{A}}(t)$ , is an indirect measure of ‘returnability’ which takes into account details of closed walks in  $\vec{S}(t)$ . In particular,  $\Psi(t)$  is a sum of all closed walks in  $\vec{S}(t)$  weighted in decreasing order by length [12].  $\Psi(t) + n$  may be thought of as the partition function of  $\vec{S}(t)$  [13].

Examining the time-series of  $\Psi(t)$  and  $\Phi(t)$  it is apparent that, unlike total net-degree, both  $\Psi(t)$  and  $\Phi(t)$  exhibit similar bursting behavior to that of  $\mu_{\text{max}}(t)$ . In particular, periods of stability ( $\mu_{\text{max}}(t) < 0$ ) generally correspond to periods when both  $\Psi(t) = 0$  and  $\Phi(t) = 0$  (for instance, in Fig. 2 this occurs  $> 90\%$  of the time). Since  $\Psi(t) = 0$  and  $\Phi(t) = 0$  if and only if  $\vec{S}(t)$  is acyclic this

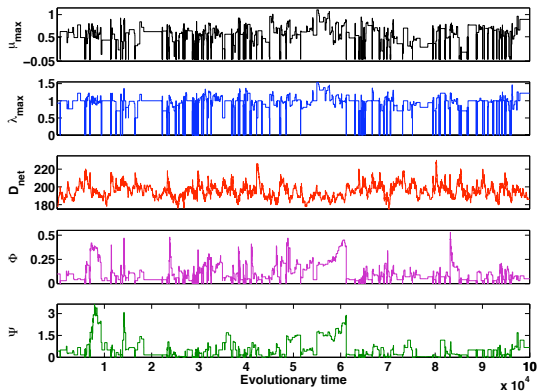


Figure 2: Evolutionary dynamics are characterized by punctuated equilibrium. Dynamics of a 100 vertex system are given. (Top) shows the time-series for  $\mu_{\max}(t)$ . Note that  $\mu_{\max}(t) = -\min \epsilon_i < 0$  when  $\vec{S}(t)$  is acyclic (in this case  $\min \epsilon_i = 6 \times 10^{-3}$ ); (Second) the time-series for  $\lambda_{\max}(t)$ , note the prevalence of 0 and +1 (and less obviously to the eye, but still present,  $\cos(\pi/l)$  for some  $l \in \mathbb{Z}^+$ ) in this series as predicted analytically; (third) the total net-degree  $D_{\text{net}}(t) = \sum_i d_{\text{net}}[v_i(t)]$ ; (fourth) the cyclic index  $\Phi(t)$ ; (bottom) the cyclic index  $\Psi(t)$ .

indicates that periods of stability occur primarily when  $\vec{S}(t)$  is acyclic. Furthermore, changes in stability predominantly occur concordantly with changes in  $\Psi(t)$  and  $\Phi(t)$  (for instance, in Fig. 2 this occurs  $> 99\%$  of the time), indicating that bursts of instability are strongly, although not exclusively, related to changes in cyclic structure (see also Fig. 3).

In order to better understand this relationship, we now derive some analytical results relating cycles and spectra of signed digraphs which will help interpret these numerics. To obtain exact results we shall focus on deriving analytic formulae for  $\Psi$  and  $\lambda_{\max}$ , and the relationship between  $\lambda_{\max}$  and  $\mu_{\max}$ , in the particular case that all cycles in  $\vec{S}$  are disjoint (that is, each vertex  $v \in V$  belongs to at most one cycle). Although this is a strong condition to impose, and most real-world networks are not expected to be cycle-disjoint, this case is analytically tractable and, since our evolutionary scheme favors the minimization of cycles, yields results which shed light on the observed dynamics. Full proofs of all analytic results are provided in Appendix A.

Firstly we observe that if a signed digraph  $\vec{S}$  is cycle-disjoint, then its spectrum has a particularly simple form. Specifically, if  $\vec{S}$  contains  $c_k^+$  positive cycles and  $c_k^-$  negative cycles of length  $k$  (for  $k = 3 \dots n$ ) [24] and all cycles are disjoint, then its spectrum is the zero eigenvalue with multiplicity  $(n - n_{\text{cyc}})$ , along with the eigenvalues of each of the cycles considered separately as induced subgraphs (that is, the union of  $c_k^+$  copies of the  $k$ -th roots of +1, and  $c_k^-$  copies of the  $k$ -th roots of -1, for  $k = 3 \dots n$ ).

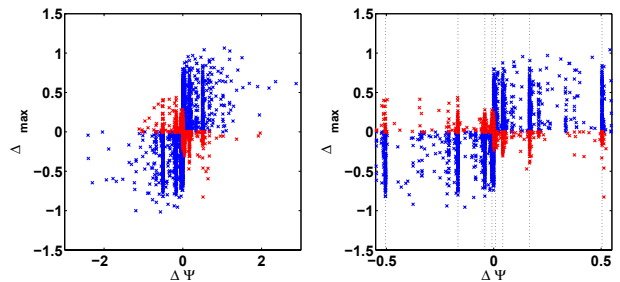


Figure 3: Transient cycles trigger bursts of instability. (left) A plot of  $\Delta\Psi(t) = \Psi(t) - \Psi(t-1)$  against  $\Delta\mu_{\max}(t) = \mu_{\max}(t) - \mu_{\max}(t-1)$  using the same data as Fig. 2. For clarity, the few changes in stability which do not occur concordantly with changes in cyclic structure are shown in light gray (red online). (Right) A close-up of the left panel. The striations arise since it is common for isolated cycles to be created or broken during the evolutionary process, triggering changes in stability. The dotted vertical lines are at  $\pm\Psi$  calculated analytically using Eq. 2 with  $k = 3 \dots 6$  and  $c_k = 1$ .

An immediate consequence of this result is that if  $\vec{S}$  is cycle-disjoint and possesses at least one positive cycle then  $\lambda_{\max} = 1$ , while if all cycles are negative then  $\lambda_{\max} = \text{Re } e^{\pi i/l} = \cos(\pi/l)$ , where  $l$  is the length of the longest cycle in  $\vec{S}$ . In this sense, positive cycles are uniformly destabilizing, while the destabilizing effect of negative cycles increases with length. Examination of time-series data shows that  $\lambda_{\max}(t) = 0, 1$  and  $\cos(\pi/l)$  for some  $3 \leq l \leq n \in \mathbb{Z}^+$ , do indeed occur commonly during evolution (for instance, in Fig. 2 this occurs  $\approx 53\%$  of the time), indicating the continual formation and breaking of isolated cycles by the evolutionary scheme.

This result is also useful since it allows us to calculate  $\Psi$  analytically in the case that  $\vec{S}$  is cycle-disjoint. In particular, if  $\vec{S}$  contains  $c_k$  ( $= c_k^+ + c_k^-$ ) disjoint cycles of length  $k$  for  $k = 3 \dots n$  then, using Eq. 1,

$$\Psi = \sum_{k=3}^n c_k H_{k,0}(1) - n_{\text{cyc}}, \quad (2)$$

where  $H_{k,0}(z)$  is the generalized hyperbolic function of order  $k$  and kind 0 [14]. Fig. 3 shows that values of  $\Psi(t)$  calculated using Eq. 2 often occur during evolution, again indicating that isolated cycles are continually formed and broken by the evolutionary scheme.

These analytical results may be used to interpret numerics by making use of two further results which relate  $\lambda_{\max}$  to  $\mu_{\max}$  in the cycle-disjoint case. Firstly, note that in the special case that  $\vec{S}(t)$  is acyclic then  $\lambda_{\max}(t) = 0$  and  $\mu_{\max}(t) = -\min \epsilon_i < 0$ , and the system is stable. Secondly, if  $\vec{S}(t)$  is cycle-disjoint then  $\mu_{\max}(t) < \lambda_{\max}(t)$  and this bound is tight ( $\mu_{\max}(t) \rightarrow \lambda_{\max}(t)$  as  $\epsilon_i \rightarrow 0$  for all  $i$ ). Consequently, if vertex dissipation (decay) rates are all small then the completion of a single cycle in an otherwise acyclic graph is sufficient to trigger a burst of instability, as seen in Fig. 2. When this occurs the evo-

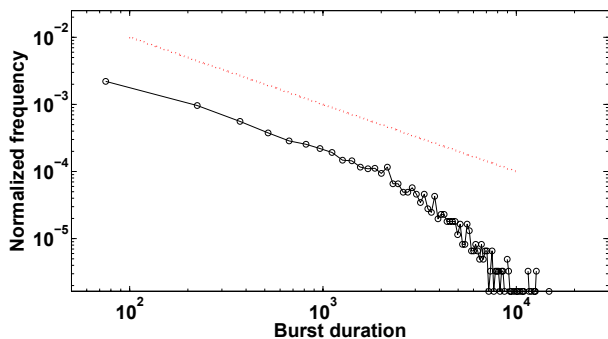


Figure 4: Bursts of instability have heavy-tailed statistics. The distribution of burst durations is shown over an interval of  $4 \times 10^6$  evolutionary time-steps for a system with 100 vertices at equilibrium. A power-law with exponent 1 is also shown for reference.

lutionary process responds by suppressing any further defective switches and rearranging local graph structure to remove the cause of the instability. Typically, this is quickly achieved and the burst of instability is relatively short. However, occasionally cycles may accumulate more rapidly than they are removed, giving rise to extended bursts of instability and heavy-tailed statistics characteristic of a critical state (see Fig. 4).

For completeness it should finally be noted that if  $\vec{S}(t)$  is not cycle-disjoint then the relationship between cycles and stability can be considerably more complex. For instance, if  $\vec{S}(t)$  is not cycle-disjoint then it is not necessarily true that  $\mu_{\max}(t) < \lambda_{\max}(t)$  and, under certain circumstances, dissipation may itself induce instability. This occurs, for instance, when positive and negative cycles intersect in a locally symmetric manner such that their contributions to the graph spectrum cancel each other out. In these cases, disparate dissipation rates may act to break the symmetry, giving rise to dissipation-induced instabilities [15]. Under these circumstances, changes in cyclic structure during the evolutionary process may not trigger concordant changes in stability. However, in practice, since they rely on rather specific structural configurations, changes in  $\mu_{\max}(t)$  which are discordant with changes in  $\Phi(t)$  and  $\Psi(t)$  are rare in our model (in Fig. 2 and Fig. 3  $> 99\%$  of changes are concordant). Nevertheless, this observation highlights the general case: stability is determined by the interplay between the cycles of  $\vec{S}(t)$ , their sign, and the relative rates of dissipation.

*Conclusions.*— Many natural systems behave in a dynamically critical manner [6, 16, 17], characterized by periods of stability (inactivity) punctuated by bursts of instability (activity). This balance between stability and instability is thought to be important since stability provides resilience in the face of inevitable environmental fluctuations by restricting long-time dynamics to localized regions of state space; while instability provides the potential for adaptability in the face of persistent en-

vironmental changes by allowing exploration of extended regions of state space. Using a simple evolutionary model we have shown that critical dynamics may emerge spontaneously and robustly due to coupling between structural rearrangement and system stability. Our results also emphasize the close relationship between cycles and dynamics, and show that arbitrarily small changes in network structure – changing the position of a single edge, for instance – can have strong and persistent effects on system dynamics.

## Appendix A: Proofs

Formal statements and proofs of results stated without proof in the main text are provided here.

Let  $\vec{S} = \vec{S}(V, E)$  be a directed signed graph with vertex-set  $V$  of size  $n$ , edge-set  $E$  of size  $m$ , no dual-edges (if  $v_i v_j \in E$  then  $v_j v_i \notin E$  for all  $i, j = 1 \dots n$ ) and no self-loops ( $v_i v_i \notin E$  for all  $i = 1 \dots n$ ). We say that  $\vec{S}$  is *cycle-disjoint* if all cycles in  $\vec{S}$  are pair-wise disjoint, that is, if every vertex participates in at most one cycle. Let  $c_k^+$  (respectively  $c_k^-$ ) be the number of positive (respectively negative) cycles of length  $k$  in  $\vec{S}$  for  $k = 3 \dots n$ . Thus, the number of vertices which participate in a cycle in  $\vec{S}$  is  $n_{\text{cyc}} = \sum_k k(c_k^+ + c_k^-)$ .

**Proposition 1.** *The eigenvalue spectrum of  $\vec{S}$  as defined above consists of the zero eigenvalue with multiplicity  $(n - n_{\text{cyc}})$  along with the union of  $c_k^+$  copies of the  $k$ -th roots of unity and  $c_k^-$  copies the  $k$ -th roots of  $-1$  for  $k = 3 \dots n$ .*

*Proof.* The proof makes use of Sachs' (coefficients) theorem (Theorem 1.32, p32 in [18]) which, for completeness, we state here in its general form.

**Theorem 1** (Sachs). *Let  $\vec{W}$  be a weighted digraph with characteristic polynomial  $z^n + a_1 z^{n-1} + \dots + a_{n-1} z + a_n$  then*

$$a_i = \sum_{L \in \mathcal{L}_i} (-1)^{p(L)} W(L), \quad (\text{A1})$$

where  $\mathcal{L}_i$  is the set of directed linear subgraphs of  $\vec{W}$  on  $i$  vertices,  $p(L)$  is the number of disjoint components in a given linear subgraph  $L$  and  $W(L)$  is the product of edge-weights over all edges in  $L$ .

We now begin our proof of Proposition 1. Let  $\mathbf{A}$  be the adjacency matrix of a cycle-disjoint signed digraph  $\vec{S}$ . The eigenvalues of  $\vec{S}$  are the solutions to the characteristic polynomial of  $\mathbf{A}$

$$z^n + a_1 z^{n-1} + \dots + a_{n-1} z + a_n. \quad (\text{A2})$$

The largest linear subgraph  $L_{\max}$  in  $\vec{S}$  consists of the disjoint union of all the cycles in  $\vec{S}$  and so has size  $n_{\text{cyc}} =$

$\sum_k k(c_k^+ + c_k^-)$ . Therefore, by Sachs' theorem  $a_i = 0$  for  $i > n_{\text{cyc}}$  and the eigenvalues of  $\vec{S}$  are solutions to

$$z^n + a_1 z^{n-1} + \dots + a_{n_{\text{cyc}}} z^{n-n_{\text{cyc}}} = 0 \quad (\text{A3})$$

$$z^{n-n_{\text{cyc}}}(z^{n_{\text{cyc}}} + a_1 z^{n_{\text{cyc}}-1} + \dots + a_{n_{\text{cyc}}}) = 0. \quad (\text{A4})$$

Thus,  $\vec{S}$  has zero as an eigenvalue with multiplicity  $(n - n_{\text{cyc}})$ . Now let

$$z^{n_{\text{cyc}}} + \tilde{a}_1 z^{n_{\text{cyc}}-1} + \dots + \tilde{a}_{n_{\text{cyc}}-1} z + \tilde{a}_{n_{\text{cyc}}} \quad (\text{A5})$$

be the characteristic polynomial of  $L_{\text{max}}$ , considered as an induced subgraph. It is immediate from the definition of  $L_{\text{max}}$  (and using Sachs' theorem) that  $\tilde{a}_i = a_i$  for all  $i$ . Thus, the additional eigenvalues of  $\vec{S}$  are the roots of Eq. A5 which are the eigenvalues of the disjoint cycles in  $L_{\text{max}}$  and the result follows.  $\square$

**Proposition 2.** *Let  $\vec{S}$  be a cycle-disjoint signed digraph with  $n$  vertices, adjacency matrix  $\mathbf{A}$  and eigenvalues  $\lambda_1, \dots, \lambda_n$ . Let  $\mathbf{b} = \text{diag}(-\epsilon_1, \dots, -\epsilon_n)$  be a diagonal matrix with  $\epsilon_i \geq 0$  for all  $i$  and let  $\mu_1, \dots, \mu_n$  be the eigenvalues of the matrix  $\mathbf{B} = \mathbf{A} + \mathbf{b}$ . Then*

$$\max_i \text{Re}(\mu_i) \leq \max_i \text{Re}(\lambda_i)$$

with equality only when  $\epsilon_i = 0$  for all  $i$ .

*Proof.* The proof consists of three parts: (1) reduction of the problem to that of a cycle; (2) proof for the positive cycle case; and (3) proof for the negative cycle case.

*Part 1: reduction of the problem to that of a cycle.* The matrix  $\mathbf{B} = \mathbf{A} + \mathbf{b}$  may be thought of as the adjacency matrix of a weighted digraph  $\vec{P}$  which has the same vertices, edges and edge-signs as  $\vec{S}$  with an additional self-loop at each vertex  $v_i \in \vec{P}$  of weight  $-\epsilon_i$ . Let  $v$  be a vertex not participating in a cycle in  $\vec{S}$ . Any linear subgraph  $L$  of  $\vec{P}$  containing  $v$  can only do so via the self-loop at  $v$  and hence  $v$  must be disjoint from all other vertices in  $L$ . Thus, removing all edges in  $\vec{P}$  which do not participate in a cycle in  $\vec{S}$ , except the weighted self-loops, creates a new graph  $\vec{Q}$  with the same linear subgraphs as  $\vec{P}$  and thus the same characteristic polynomial as  $\vec{P}$  by Sachs' theorem. The graph  $\vec{Q}$  consists of the disjoint union of the perturbed cycles of  $\vec{S}$  and  $(n - n_{\text{cyc}})$  isolated vertices each with a self-loop of weight  $-\epsilon_i$  for some  $i$ . Each of the isolated vertices contributes the eigenvalue  $-\epsilon_i < 0$  for some  $i$  to the spectrum of  $\vec{Q}$ . The remainder of the spectrum is determined by the disjoint union of perturbed cycles in  $\vec{Q}$ . Since the spectrum of a disjoint union of graphs is the union of the spectra of each of the components, it is therefore sufficient to prove the proposition for  $\vec{S}$  a cycle. In particular, if  $\vec{S}$  is acyclic then the spectra of  $\vec{P}$  is just the set  $\{-\epsilon_i \mid i = 1 \dots n\}$  which has maximal real-part  $-\min \epsilon_i < 0$  as stated in the main text.

*Part 2: proof for the positive cycle case.* Let  $\vec{C}_n^+$  be a positive cycle with  $n$  vertices and adjacency matrix  $\mathbf{A}$ . The characteristic polynomial of  $\vec{C}_n^+$  is  $z^n - 1$  and the eigenvalues of  $\vec{C}_n^+$  are therefore the  $n$ th roots of unity, which have maximal real-part 1 for any  $n$ . The adjacency matrix of a perturbed positive cycle is  $\mathbf{A} + \text{diag}(-\epsilon_1, \dots, -\epsilon_n)$ , which has characteristic polynomial (cf. Eq. A1)

$$p_n^+(z) = (z + \epsilon_1) \cdot (z + \epsilon_2) \cdot \dots \cdot (z + \epsilon_n) - 1 = \prod_{i=1}^n (z + \epsilon_i) - 1.$$

Thus, we need to prove that every root  $\lambda$  of  $p_n^+$  satisfies  $\text{Re}(\lambda) < 1$  when at least one  $\epsilon_i \in \mathbb{R}$  is nonzero. From now on we shall assume, without loss of generality, that  $\epsilon_1 > 0$ .

We shall use Rouché's theorem, a well-known theorem in complex analysis for locating the roots of functions. For a proof of Rouché's theorem see [20].

**Theorem 2 (Rouché).** *Let  $f$  and  $g$  be holomorphic functions in a domain  $R \subset \mathbb{C}$ . Let  $D \subset R$  be a bounded subset such that its boundary  $\partial D$  is a simple closed curve null-homologous inside  $R$ . If*

$$|f(z) - g(z)| < |f(z)| \text{ for all } z \in \partial D \quad (\text{A6})$$

then  $f$  and  $g$  have the same number of zeros inside  $D$ .

To apply Rouché's theorem we take

$$f(z) = \prod_{i=1}^n (z + \epsilon_i)$$

$$g(z) = p_n^+(z)$$

and we will define  $D$  in a moment. It is immediate that  $|f(z) - g(z)| = 1$  for all  $z \in \mathbb{C}$ . Let  $\epsilon_i$  be the ball of radius 1 centered at  $-\epsilon_i$  for each  $i$  and  $\mathcal{B} = \bigcup_i \epsilon_i$  be the union of the balls. Then

$$|f(z)| = \prod_{i=1}^n |z + \epsilon_i| > 1 \quad \text{if } z \notin \mathcal{B}. \quad (\text{A7})$$

Now  $f(t)$  with  $t \in [0, 1]$  is a strictly increasing real function with  $f(1) = \prod_{i=1}^n (1 + \epsilon_i) \geq 1 + \epsilon_1 > 1$  so there exists  $0 \leq t_0 < 1$  with  $f(t_0) > 1$ . Indeed

$$|f(z)| > 1 \quad \text{for all } z \in \mathbb{C} \text{ with } \text{Re}(z) = t_0. \quad (\text{A8})$$

To see this, let  $z \in \mathbb{C}$  with  $\text{Re}(z) = t_0$  and  $\text{Im}(z) = y$ . Then

$$|z + \epsilon_i| = \sqrt{(t_0 + \epsilon_i)^2 + y^2} \geq \sqrt{(t_0 + \epsilon_i)^2} = |t_0 + \epsilon_i|$$

for all  $i = 1, \dots, n$  and thus  $|f(z)| \geq |f(t_0)| > 1$ .

Finally, let  $a > 1$  and  $b < \min_i \{-\epsilon_i - 1\}$  and define

$$D = \{z \in \mathbb{C} \mid b \leq \text{Re}(z) \leq t_0 \text{ and } -a \leq \text{Im}(z) \leq a\}.$$

Then for all  $z \in \partial D$  we have either  $\text{Re}(z) = t_0$  or  $z \notin \mathcal{B}$  so  $|f(z)| > 1 = |f(z) - g(z)|$  by Eq. A7 and Eq. A8.

Therefore Rouché's Theorem gives that  $f(z)$  and  $g(z)$  both have all their roots inside  $D$ . In particular, any root  $\lambda$  of  $g(z) = p_n^+(z)$  satisfies  $\text{Re}(\lambda) < t_0 < 1$  and this proves the positive case.

**Remark 1.** Note that, in addition, any root of  $p_n^+(z)$  with positive real-part must lie *strictly* inside the unit circle. To see this, observe that if  $|z| = 1$  then  $|f(z)| = \prod_i |z + \epsilon_i| \geq |z + \epsilon_1| > 1$  so  $z$  is not a root of  $p_n^+(z)$  by the same argument. We shall make use of this observation in a moment.

**Remark 2.** The positive case may also be proven by application of a modification of Geršgorin's disc theorem due to Brualdi (see Theorem 6.4.18 in [19]).

*Part 3: proof for the negative cycle case.* Let  $\vec{C}_n^-$  be a negative cycle with  $n$  vertices and adjacency matrix  $\mathbf{A}$ . The characteristic polynomial of  $\vec{C}_n^-$  is  $z^n + 1$  and the eigenvalues of  $\vec{C}_n^-$  are therefore the  $n$ th roots of  $-1$ , which have maximal real-part  $\cos(\pi/n)$ . The adjacency matrix of a perturbed negative cycle is  $\mathbf{A} + \text{diag}(-\epsilon_1, \dots, -\epsilon_n)$ , which has characteristic polynomial (cf. Eq. A1)

$$p_n^-(z) = (z + \epsilon_1) \cdot (z + \epsilon_2) \cdot \dots \cdot (z + \epsilon_n) + 1 = \prod_{i=1}^n (z + \epsilon_i) + 1.$$

Thus, we need to prove that every root  $\lambda$  of  $p_n^-$  satisfies  $\text{Re}(\lambda) < \cos(\pi/n)$ , when at least one  $\epsilon_i \in \mathbb{R}$  is nonzero. Again assume, without loss of generality, that  $\epsilon_1 > 0$ .

We first note that by exactly the same argument as the positive case, we can prove that all the roots  $\lambda$  of  $p_n^-(z)$  satisfy  $\text{Re}(\lambda) < 1$  and (by Remark 1) that any root of  $p_n^-(z)$  with positive real-part must lie strictly inside the unit circle. However, in the negative case this bound is not sufficiently tight to prove the result since the magnitude of the maximal real-part of the eigenvalues depends upon the length of the cycle. In fact, we require the tightest possible bound and the proof in the negative case is correspondingly more involved than that of the positive case.

We shall progress as before. However this time we use a strengthened version of Rouché's Theorem [20, p. 390] in which the inequality in Eq. A6 is replaced by the inequality

$$|f(z) - g(z)| < |f(z)| + |g(z)| \text{ for all } z \in \partial D. \quad (\text{A9})$$

In this case, we use the functions

$$\begin{aligned} f(z) &= z^n + 1, \\ g(z) &= p_n^-(z). \end{aligned}$$

and the region

$$D_\theta = \{z = re^{i\varphi} \in \mathbb{C} \mid 0 \leq r \leq 1, -\theta \leq \varphi \leq \theta\}$$

where  $0 < \theta < \pi/n$ . In particular, we shall prove that

$$|f(z) - g(z)| < |f(z)| + |g(z)| \text{ for all } z \in \partial D_\theta$$

from which it follows that  $p_n^-(z)$  has the same number of roots that  $f(z)$  in  $D_\theta$ . Since, by construction,  $f(z)$

has no roots in  $D_\theta$  this implies that all roots  $\lambda$  of  $p_n^-(z)$  with positive real-part must lie strictly in the unit circle excluding the region  $D_\theta$  for all  $0 < \theta < \pi/n$  and, in particular, that each root  $\lambda$  of  $p_n^-(z)$  has real-part less than  $\cos(\pi/n)$ .

First note that in general

$$\begin{aligned} |f(z)| + |g(z)| &= |f(z)| + |g(z) - f(z) + f(z)| \\ &\geq |f(z)| + |g(z) - f(z)| - |f(z)| \\ &= |g(z) - f(z)| \end{aligned}$$

so the non-strict inequality holds for every  $z \in \mathbb{C}$  (observe that equality holds, for instance, for any root of either  $f$  or  $g$ ). We therefore only need to demonstrate that

$$|f(z) - g(z)| \neq |f(z)| + |g(z)| \text{ for all } z \in \partial D_\theta \quad (\text{A10})$$

and the result is proven. To do so, we make use of the following two lemmas, whose proofs we leave to the end.

**Lemma 1.** *Let  $u, v \in \mathbb{C}$ . Then*

$$|u| = |u + v| + |v| \quad (\text{A11})$$

*if and only if either  $u = v = 0$  or  $v = \alpha u$  with  $0 \leq \alpha \leq -1$ .*

Consider the (open) upper and lower half-planes

$$\begin{aligned} H^+ &= \{z \in \mathbb{C} \mid \text{Im}(z) > 0\}, \\ H^- &= \{z \in \mathbb{C} \mid \text{Im}(z) < 0\}, \end{aligned}$$

and the four (open) quadrants

$$Q_k = \{z = re^{i\varphi} \in \mathbb{C} \mid r > 0, \frac{(k-1)\pi}{2} < \varphi < \frac{k\pi}{2}\}$$

for  $k = 1 \dots 4$ . Additionally, for a nonzero complex number  $w$  write  $\text{Arg}(w)$  for the unique  $\varphi \in (-\pi, \pi]$  such that  $w = |w|e^{i\varphi}$ .

**Lemma 2.** *Let  $b \in \mathbb{R}^+$ .*

1. *If  $z \in Q_1$  then  $|z+b| > |z| > 0$  and  $0 < \text{Arg}(z+b) < \text{Arg}(z)$ .*
2. *Suppose that  $w_1, w_2 \in H^+$  satisfy  $|w_1| > |w_2|$  and  $\text{Arg}(w_1) < \text{Arg}(w_2)$ . Then either  $w_1 - w_2 \in H^+$  or  $w_1 - w_2 \in Q_4 \cup \mathbb{R}^+$ .*

We now apply Lemma 1 and Lemma 2 to complete the proof.

Divide  $D_\theta$  into three regions:

$$D_\theta^+ = D_\theta \cap H^+, \quad D_\theta^- = D_\theta \cap H^- \text{ and } D_\theta \cap \mathbb{R}.$$

Let  $z \in D_\theta^+$ . To make use of Lemma 1 set  $u = s_{n-1}z^{n-1} + \dots + s_1z + s_0$  and  $v = z^n + 1$ . We argue by contradiction. Suppose that  $z$  does not satisfy Eq. A10, that is, in terms of  $u$  and  $v$

$$|u| = |u + v| + |v|. \quad (\text{A12})$$

Therefore by Lemma 1  $u$  and  $v$  lie on a line through the origin. We shall prove that  $v \in Q_1$  and  $u \notin Q_3$  and hence arrive at a contradiction.

We know that for  $z \in D_\theta$ ,  $0 < \text{Arg}(z) \leq \theta < \pi/n$  and  $|z| \leq 1$  hence  $0 < \text{Arg}(z^n) < \pi$  and  $|z^n| \leq 1$ . Consequently  $v = z^n + 1 \in Q_1$ . On the other hand, consider

$$u = s_{n-1}z^{n-1} + \dots + s_1z + s_0 = \prod_{i=1}^n(z + b_i) - z^n.$$

Write  $w_1 = \prod_{i=1}^n(z + b_i)$  and  $w_2 = z^n$ . By Lemma 2 (1),  $|w_1| > |w_2|$  and  $0 < \text{Arg}(w_1) < \text{Arg}(w_2)$  since at least  $b_1 > 0$ . By Lemma 2 (2),  $u = w_1 - w_2$  lies in either  $H^+$  or  $Q_4 \cup \mathbb{R}^+$  and thus  $u \notin Q_3$ .

If  $z \in D_\theta^-$ , we apply exactly the same argument to the complex conjugate  $\bar{z} \in D_\theta^+$  to conclude that  $\bar{u}$  and  $\bar{v}$  do not lie in a line through the origin, therefore neither do  $u$  and  $v$ , again contradicting Lemma 1.

Finally, if  $z \in D_\theta \cap \mathbb{R} = [0, 1]$  then  $u$  and  $v$  are both positive real and hence do not satisfy Lemma 1 and this completes the proof.  $\square$

*Proof of Lemma 1.* Write  $u = a + bi$ ,  $v = c + di$ . Then  $|u + v| = |v| - |u|$  means

$$\sqrt{(a+c)^2 + (b+d)^2} = \sqrt{c^2 + d^2} - \sqrt{a^2 + b^2}$$

which implies that (squaring and simplifying)

$$ac + bd = \sqrt{(a^2 + b^2)(c^2 + d^2)}.$$

Squaring and simplifying again we obtain

$$(ad - bc)^2 = 0, \text{ that is, } ad = bc.$$

If  $u = 0$  then Eq. A11 implies  $v = 0$ . If  $u \neq 0$  then either  $\alpha = d/b$  or  $\alpha = c/a$  is well-defined and satisfies  $v = \alpha u$ .

In addition,

$$|u| = |u + v| + |v| = |u + \alpha u| + |\alpha u| \Rightarrow 1 = |1 + \alpha| + |\alpha|$$

and a case study shows that  $\alpha \leq 0$  and  $1 + \alpha \geq 0$ , that is,  $-1 \leq \alpha \leq 0$ . One finally checks that, for such an  $\alpha$ ,  $v = \alpha u$  satisfies Eq. A11.  $\square$

*Proof of Lemma 2.* (1) Let  $z = x + iy$  with  $x, y > 0$ . Then

$$|z + b| = \sqrt{(x+b)^2 + y^2} > \sqrt{x^2 + y^2} = |z|$$

since  $x + b > x > 0$ . Recall that arctan is a strictly increasing function. Thus

$$\text{Arg}(z + b) = \arctan\left(\frac{y}{x+b}\right) < \arctan\left(\frac{y}{x}\right) = \text{Arg}(z).$$

(2) Let  $w_1 = x_1 + iy_1$  and  $w_2 = x_2 + iy_2$ . If  $y_1 > y_2$  then  $\text{Im}(w_1 - w_2) = y_1 - y_2 > 0$  so  $w_1 - w_2 \in H^+$ . Suppose that  $y_2 \geq y_1 > 0$  (the reader should draw a picture at this stage to convince themselves). Since  $|w_1| > |w_2|$  we have  $x_1^2 - x_2^2 > y_2^2 - y_1^2 \geq 0$ , that is,  $x_1^2 > x_2^2$  or, equivalently,  $|x_1| > |x_2|$ . Then either (a)  $x_1 > |x_2|$  or (b)  $x_1 < -|x_2|$ . The latter is impossible: if  $x_2 \geq 0$  then  $0 < \text{Arg}(w_2) \leq \pi/2$  but  $x_1 < -x_2 \leq 0$  so  $\text{Arg}(w_1) > \pi/2$ ; if  $x_2 < 0$  then  $x_1 < x_2 < 0$  and hence

$$\frac{1}{x_2} < \frac{1}{x_1} \Rightarrow \frac{y_2}{x_2} < \frac{y_1}{x_1} \Rightarrow \text{Arg}(w_2) < \text{Arg}(w_1).$$

In either case the condition  $\text{Arg}(w_1) < \text{Arg}(w_2)$  is contradicted. So we must have (a)  $x_1 > |x_2|$ , that is,  $x_1 - x_2 > 0$  and therefore

$$w_1 - w_2 = (x_1 - x_2) + (y_1 - y_2)i \in Q_4 \cup \mathbb{R}^+. \quad \square$$

- 
- [1] R. Albert and A.-L. Barabási, Rev. Mod. Phys. **74**, 47 (2002).
- [2] M. E. J. Newman, SIAM Rev. **45**, 167 (2003).
- [3] R. M. May, Nature **238**, 413 (1972).
- [4] R. Thomas and R. D'Ari, *Biological feedback* (CRC Press, 1990).
- [5] T. Gross and B. Blasius, J. R. Soc. Interface **5**, 259 (2008).
- [6] D. Garlaschelli, A. Capocci, and G. Caldarelli, Nat. Phys. **3**, 813 (2007).
- [7] T. Zaslavsky, Discr. Appl. Math. **4**, 47 (1982).
- [8] A. Ma'ayan, G. A. Cecchi, J. Wagner, A. R. Rao, R. Iyengar, and G. Stolovitzky, Proc. Natl. Acad. Sci. USA **105**, 19235 (2008).
- [9] A.-L. Barabási and R. Albert, Science **286**, 509 (1999).
- [10] M. Batty, Nature **444**, 592 (2006).
- [11] A. Gautreau, A. Barrat, and M. Barthélemy, Proc. Nat. Acad. Sci. USA **106**, 8847 (2009).
- [12] E. Estrada and N. Hatano, Linear Algebra and Its Applications **430**, 1886 (2009).
- [13] E. Estrada and N. Hatano, Chem. Phys. Lett. **439**, 247 (2007).
- [14] A. Ungar, Amer. Math. Month. **89**, 688 (1982).
- [15] R. Krechetnikov and J. E. Marsden, Rev. Mod. Phys. **79**, 519 (2007).
- [16] P. Bak, *How nature works: the science of self-organized criticality* (Springer-Verlag, 1999).
- [17] M. O. Magnasco, O. Piro, and G. A. Cecchi, Phys. Rev. Lett. **102**, 258102 (2009).
- [18] D.M. Cvetković, M. Doob, and H. Sachs. *Spectra of graphs: theory and applications*. Academic Press, 1980.
- [19] R. A. Horn and C. R. Johnson. *Matrix analysis*. Cambridge University Press, 1990.
- [20] R. Remmert. *Theory of complex functions*. Springer-verlag, 1998.
- [21] For computational efficiency in the simulations shown we set the edge-inclusion probability  $\approx \ln(n)/n$  and consider a maximally sparse connected random graph. Qualita-

tively the same results may be achieved for more dense graphs.

- [22] That is, after an initial transient ‘settling-down’ period ( $4 \times 10^6$  time-steps prior to data shown).
- [23] Recall that a cycle of length  $k$  is a non-intersecting path

of length  $k$  from a vertex back to itself respecting edge directions.

- [24] A cycle  $c$  is positive (negative) if the product of the edge signs in  $c$  equals  $+1$  ( $-1$ ).